IOP Publishing Nanotechnology

Nanotechnology **25** (2014) 055206 (5pp) doi:10.1088/0957-4484/25/5/055206

Electroluminescence from graphene excited by electron tunneling

Ryan Beams[1], **Palash Bharadwaj**[2] **and Lukas Novotny**[2]

[1] Institute of Optics, University of Rochester, Rochester, NY 14627, USA
[2] ETH Zürich, Photonics Laboratory, 8093 Zürich, Switzerland

E-mail: lnovotny@ethz.ch

Received 17 October 2013, revised 5 December 2013
Accepted for publication 12 December 2013
Published 9 January 2014

Abstract

We use low-energy electron tunneling to excite electroluminescence in single layer graphene. Electrons are injected locally using a scanning tunneling microscope and the luminescence is analyzed using a wide-angle optical imaging system. The luminescence can be switched on and off by inverting the tip–sample bias voltage. The observed luminescence is explained in terms of a hot luminescence mechanism.

Keywords: graphene, electron tunneling, photoemission, electroluminescence, scanning tunneling microscopy

(Some figures may appear in colour only in the online journal)

1. Introduction

Graphene-based optoelectronics show considerable promise due to the linear dispersion, tunable Fermi level, and nearly flat absorption profile of graphene [1–3]. Using these properties, graphene photodetectors have been demonstrated by decorating graphene flakes with metal structures [4–6], quantum dots [7], and by exciting plasmons in graphene [8, 9]. While graphene optoelectronics has largely concentrated on converting photons into electrons, the reverse process also provides insight into carrier dynamics. For example, electroluminescence (EL) studies of carbon nanotubes (CNTs) have explored thermal, phonon–electron, and electron–electron processes [10–15]. However, very few EL measurements have been performed on graphene. These measurements have either been limited to multilayer flakes [14] or nano-crystal mediated processes [16].

In this work we use a scanning tunneling microscope (STM) to inject carriers into a graphene flake and study the resulting luminescence in ambient conditions. While STM-based EL has been observed in CNTs [13, 12], previous attempts on graphite have been unsuccessful [12]. We find that the luminescence depends on the energy of the injected carriers as well as the number of graphene layers. This is consistent with a hot luminescence mechanism. To the best of our knowledge this is the first demonstration of STM-induced EL from single layer graphene.

2. Results and discussion

STM light emission in metals is well-established [17–19]. In noble metals it originates from tunneling electrons exciting a localized plasmon mode in the gap between the tip and metal surface, known as a gap plasmon. The gap plasmon can lead to light emission by either decaying directly into a photon or by coupling to a surface plasmon [19–21]. Plasmons have also been demonstrated in graphene [22–24]. However to excite plasmons in graphene the Fermi level, E_F, must be shifted such that $E_F > \hbar\omega$, where $\hbar\omega$ is the energy of the plasmon [25]. Due to this requirement combined with the technical challenges of doping graphene by more than 1 eV, graphene plasmonics has focused on the infrared (IR) spectral range. To generate tunneling-induced light emission at visible wavelengths we therefore have to explore other interaction mechanisms.

The process that we exploit in this work is hot luminescence (HL). For an undoped graphene flake an incident photon can excite an electron–hole pair. Since there are no available states in the valence band the electron will either recombine almost instantaneously with the created

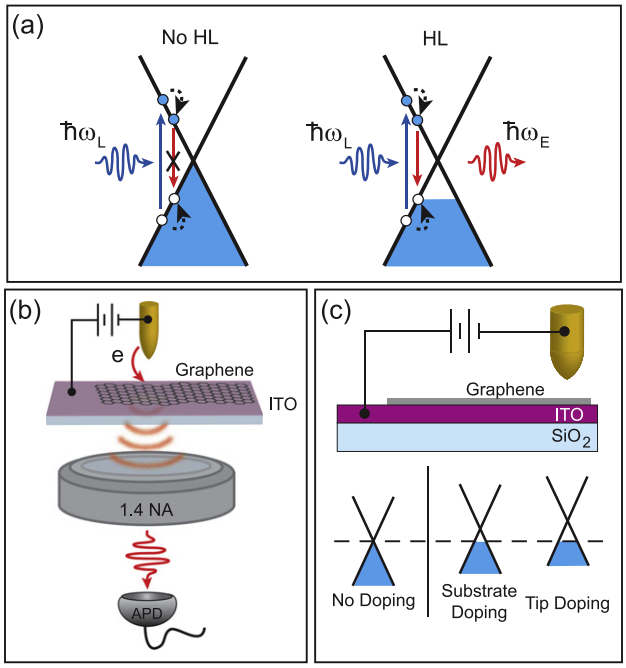

Figure 1. (a) Diagram of the hot luminescence mechanism (HL). An incident photon ($\hbar\omega_L$) excites an electron–hole pair. If the graphene is undoped (left panel), the electron–hole pair combines non-radiatively and HL is not observed. Under correct doping conditions the electron–hole pair can recombine and emit a photon ($\hbar\omega_E$), see right panel. (b) Sketch of the doping mechanisms for the graphene flake due to the tip and the substrate. The case without doping is shown as a reference. (c) Sketch of the experimental setup. The graphene sample is mounted on an piezo-scan-stage on top of an inverted microscope. A STM scan-head incorporating an Au tip is placed on top of the microscope for topographic and luminescence imaging. The resulting luminescence is collected with a 1.4 NA microscope objective and sent to an avalanche photodiode (APD).

hole, as in the case of Raman and Rayleigh scattering, or recombine non-radiatively. If the flake is doped appropriately, the graphene can still absorb an incident photon and there will also be available states for the carriers to recombine and emit a red-shifted photon [26]. In this case the new radiative decay channel dominates over Raman processes, as shown in [26]. Figure 1(a) shows a sketch of the process. This process also requires that a graphene flake is doped, but the required doping level is much lower than for plasmons. The doping-induced Fermi level must be in the range $\hbar\omega_L > 2|E_F| \geq \hbar\omega_E$, where $\hbar\omega_L$ and $\hbar\omega_E$ are the photon energy of the laser and the emission, respectively [26]. This process can be translated to an STM picture by replacing the incident photon with an injected electron. In this case, the energy of the injected electron (or hole) can be controlled by the bias voltage V_B.

Figure 1(b) shows a sketch of the experimental setup. A graphene flake was exfoliated onto an indium–tin-oxide (ITO) coated coverslip and placed on an inverted microscope. A home-built STM scan-head incorporating an electrochemically etched gold tip was placed on top of the microscope. The tip was positioned into the focus of a 1.4 NA oil immersion microscope objective, which is used for collecting the EL and sending it to an avalanche photodiode (APD). The sample was placed on a piezo-scan-stage that scanned the sample underneath the STM tip to form simultaneous topographic and luminescence images. For STM measurements the tip was grounded and a bias of $V_B = \pm 2$–3 V was applied to the sample. The tunneling current, I_t, was kept constant at 1 nA, corresponding to a tip–sample separation of ~1 nm.

The observation of HL in graphene requires doping. Figure 1(c) shows three different regimes of doping, corresponding to no doping, substrate doping, and tip doping [29]. The Fermi level of the graphene flake can also be altered by placing the graphene flake on a substrate with a different work function. In our case we used an oxygen-plasma cleaned ITO coated glass substrate, which leads to a p-doped graphene flake [27, 28]. Based on the work functions, this type of contact doping can be as large as ~0.5 eV. Additionally, the STM tip gives rise to band-bending in the graphene due to two mechanisms. First, the work function difference between the tip material and the graphene leads to local doping of the graphene flake. For example, an Au tip in combination with graphene gives rise to a p-doping due to the higher work function of the Au tip [29]. Second, the bias voltage V_B gives rise to a capacitive effect. For the bias voltages used in our measurements, these two mechanisms lead to graphene doping of ~0.5–0.65 eV [29], which is sufficient to observe HL at visible or near-IR wavelengths.

Since the graphene flake is p-doped it should be possible to observe HL when electrons are injected, as illustrated in figure 2(a). The resulting image is shown in figure 2(b) and it clearly shows EL from the graphene flake. However, when V_B is changed to inject holes instead of electrons (figure 2(c)) the luminescence disappears as shown in figure 2(d). This measurement is in agreement with the proposed HL mechanism. Count rates of ~2 kc s^{-1} were recorded, corresponding to an electron-to-photon conversion efficiency of ~10^{-6}. The background in figure 2(d) originates from the radiative decay of plasmons in the Au tip that were excited by electrons tunneling from the substrate into the tip. To verify that the sample was not altered by injecting holes, an additional electron injection image was acquired, which turned out to be in agreement with figure 2(b). Additionally Raman spectra were acquired before and after the STM measurements and no disorder-induced D band scattering was observed indicating that the process is not related to defects and it is not damaging the flake [30, 31]. We note that [12] and [10] observed STM light emission from multi-wall carbon nanotubes using $I_t = 10$–50 nA, compared to $I_t = 1$ nA used in the present work. The authors argued that the emission was related to Van Hove singularities or local defects; neither of these effects can explain the observed luminescence in graphene.

The HL mechanism in graphene is different from the plasmon-induced mechanism observed in noble metals. Unlike metals, HL in graphene does not require an intermediate plasmon mode, such as a gap plasmon, for momentum conservation. To illustrate this, similar HL images were taken using a tungsten tip, which does not support

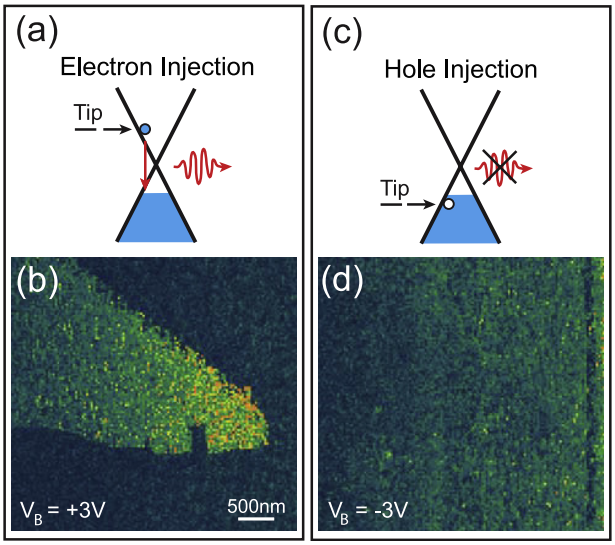

Figure 2. Sketch of the HL mechanism and the measurements. The graphene flake is p-doped due to the tip and substrate. (a) Electrons are injected and inter-band transitions are allowed. (b) HL image of the flake when electrons are injected. (c) Holes are injected, but inter-band transitions are forbidden. (d) HL image of the flake when holes are injected.

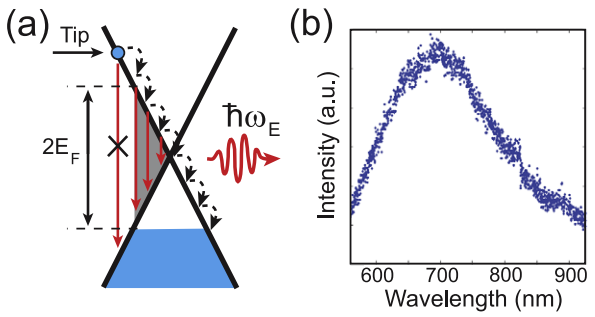

Figure 3. (a) Sketch of the HL process. The gray shaded area represents the electron energies that can radiative recombine. Electrons above $2E_F$ cannot radiatively decay without first losing energy through an non-radiative process, represented by the dashed arrows. (b) Spectrum of the HL from the graphene flake shown in figure 2. For this measurement $V_B = +3$ V.

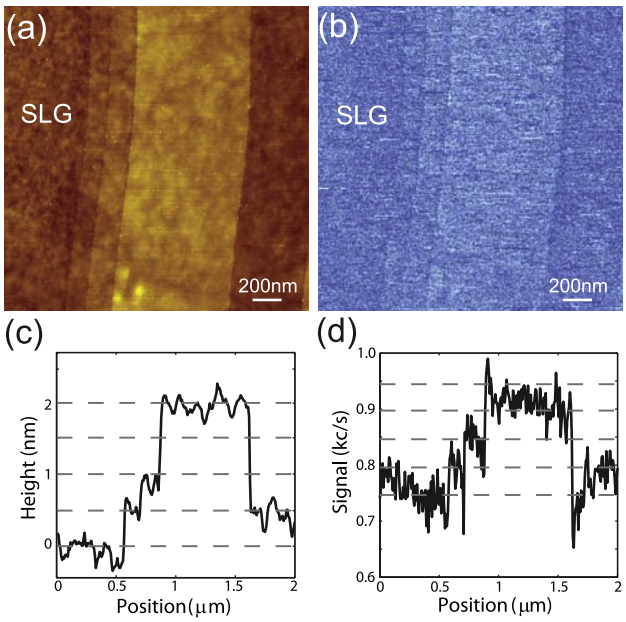

Figure 4. Dependence of HL on the number of layers. (a) Topographic image of a graphene flake showing different numbers of layers. (b) Corresponding STM hot luminescence image also showing the layers. SLG = single layer graphene. (c) Topographic profile from (a). The horizontal lines are spaced by 0.5 nm. (d) Luminescence profile from (b). The horizontal dashed lines are spaced by 50 c s^{-1}. For these measurements $V_B = +2$ V and $I_t = 2$ nA.

plasmons (data not shown). For STM in graphene, electrons inelastically tunnel to states on the Dirac-cone near the **K**-point by creating an acoustic phonon [32, 29]. From this excited state near the **K**-point, the hot electron can relax through a variety of pathways including HL. The sketches in figures 2(a) and (c) ignore the initial phonon scattering event since it is not relevant for the mechanism being presented. The HL process competes with three non-radiative decay channels each with a characteristic time-scale: electron–electron scattering (∼10 fs), electron–phonon scattering (∼200 fs), and electron–lattice cooling (>1 ps) [33–35]. As can be seen from figure 2(b), the HL is highly localized and this localization is determined by the decay rate of the carriers. The HL was found to be localized to <25 nm, as can be seen from the sharpness of the edges in figure 4(d). If the HL process was not highly localized, then the injected electrons could travel some distance before radiatively decaying. This would result in a blurring of the edges in the HL images compared to the topography, which is not seen. Using the Fermi velocity in graphene ($v_F \sim 10^6$ m s^{-1}), this localization leads to a decay time for the HL process of ∼25 fs, which suggests that electron–electron scattering is the primary mechanism competing with the radiative recombination of injected carriers.

To further study the HL mechanism a spectrum was acquired from the graphene flake shown in figure 2. As discussed above, HL can be observed for energies $\leq 2E_F$, represented by the gray shaded area in figure 3(a). If the energy of the injected electron is less than $2E_F$, the electron must first lose energy before radiatively decaying. The HL process is competing with other processes, such as electron–electron scattering, which is represented by the dashed arrows in figure 3(a). The spectrum is shown in figure 3(b). As expected the spectrum has a long tail into the IR, which qualitatively agrees with the optically excited HL presented in [26]. Since this sample was prepared on ITO both the substrate and tip doping are present, which is sufficient to lead to the observed HL.

HL is an inter-band process and as such the strength of the signal should scale with the number of layers. The most prevalent example of this is the 2.3% absorption per layer in graphene [2]. To determine the scaling of the HL signal with the number of layers an additional sample was prepared. In this case the flake was exfoliated onto a glass coverslip and a platinum electrode was evaporated onto one side of the flake. The doping from the electrode is negligible because

of the large separation distance between the electrode and the measurement location [36, 29]. As before, the sample was p-doped due to the Au tip and electrons were injected via tunneling. Figure 4(a) shows the topographic image of a flake with different numbers of layers. The entire image was acquired on the flake and the single layer graphene (SLG) area is labeled. The HL image is shown in figure 4(b). Interestingly, the number of layers shown in the topography is also visible in the HL image. Horizontal profiles from the topography and HL are shown in figures 4(c) and (d). Since the signal-to-noise ratio was low the top parts of the images were binned vertically. The horizontal dashed lines are spaced by 0.5 nm and 50 c s^{-1} in figure 4(c) and figure 4(d), respectively. The topographic step height is slightly larger than expected for graphene and is likely due to calibration errors of the scan-head. These profiles illustrate that the HL signal scales linearly with the number of layers and provides strong evidence that the EL mechanism is an inter-band process, as expected.

3. Summary

In conclusion, we have demonstrated high-resolution graphene luminescence excited by electron tunneling. The luminescence signal depends on the bias voltage V_B and scales with the number of graphene layers. Our observations are in tune with a hot luminescence mechanism, which can be controlled by local doping. Because tunneling-induced hot luminescence depends on doping, our technique can be employed for recording spatial maps of the relative Fermi level. In comparison to Kelvin probe force microscopy, this technique would allow for the local photon properties to be correlated with the relative Fermi level at that location. This technique would provide insight into the radiative decay pathways of graphene-based devices. By using mid-infrared detectors, our technique can also be used to electrically excite plasmons in graphene.

Acknowledgments

We thank Victor Brar, Ado Jorio, Gustavo Cançado, and Nick Vamivakas for the helpful discussions. We are grateful for financial support by the US Department of Energy (grant DE-FG02-05ER46207).

References

[1] Geim A K and Novoselov K S 2007 The rise of graphene *Nature Mater.* **6** 183
[2] Nair R R, Blake P, Grigorenko A N, Novoselov K S, Booth T J, Stauber T, Peres N M R and Geim A K 2008 Fine structure constant defines visual transparency of graphene *Science* **320** 1308
[3] Mak K F, Sfeir M Y, Wu Y, Lui C H, Misewich J A and Heinz T F 2008 Measuring of the optical conductivity of graphene *Phys. Rev. Lett.* **101** 196405
[4] Echtermeyer T J, Britnell L, Jasnos P K, Lombardo A, Gorbachev R V, Grigorenko A N, Geim A K, Ferrari A C and Novoselov K S 2011 Strong plasmonic enhancement of photovoltage in graphene *Nature Commun.* **2** 458
[5] Fang Z, Wang Y, Liu Z, Schlather A, Ajayan P M, Koppens F H L, Nordlander P and Halas N J 2012 Plasmon-induced doping of graphene *ACS Nano* **6** 10222–8
[6] Fang Z, Liu Z, Wang Y, Ajayan P M, Nordlander P and Halas N J 2012 Graphene-antenna sandwich photodetector *Nano Lett.* **12** 3808–13
[7] Konstantatos G, Badioli M, Gaudreau L, Osmond J, Bernechea M, Pelayo Garcia de Arquer F, Gatti F and Koppens F H L 2012 Hybrid graphene-quantum dot phototransistors with ultrahigh gain *Nature Nanotech.* **7** 363–8
[8] Fang Z, Thongrattanasiri S, Schlather A, Liu Z, Ma L, Wang Y, Ajayan P M, Nordlander P, Halas N J and Javier Garca de Abajo F 2013 Gated tunability and hybridization of localized plasmons in nanostructured graphene *ACS Nano* **7** 2388–95
[9] Ju L *et al* 2011 Graphene plasmonics for tunable terahertz metamaterials *Nature Nanotech.* **6** 630–4
[10] Coratger R, Salvetat J-P, Carladous A, Ajustron F, Beauvillain J, Bonard J-M and Forró L 2001 STM induced luminescence in carbon nanotubes *Eur. Phys. J. Appl. Phys.* **15** 177–80
[11] Mann D, Kato Y K, Kinkhabwala A, Pop E, Cao J, Wang X, Zhang L, Wang Q, Guo J and Dai H 2007 Electrically driven thermal light emission from individual single-walled carbon nanotubes *Nature Nanotech.* **2** 33–8
[12] Uemura T, Yamaguchi S, Akai-Kasaya M, Saito A, Aono M and Kuwahara Y 2006 Tunneling-current-induced light emission from individual carbon nanotubes *Surf. Sci.* **600** L15–9
[13] Misewich J A, Martel R, Avouris Ph, Tsang J C, Heinze S and Tersoff J 2003 Electrically induced optical emission from a carbon nanotube FET *Science* **300** 783
[14] Essig S *et al* 2010 Phonon-assisted electroluminescence from metallic carbon nanotubes and graphene *Nano Lett.* **10** 1589–94
[15] Rai P, Hartmann N, Berthelot J, Arocas J, des Francs G C, Hartschuh A and Bouhelier A 2013 Electrical excitation of surface plasmons by an individual carbon nanotube transistor *Phys. Rev. Lett.* **111** 026804
[16] He C *et al* 2013 Tunable electroluminescence in planar graphene/SiO_2 memristors *Adv. Mater.* **25** 5593–8
[17] Gimzewski J K, Reihl B, Coombs J H and Schlittler R R 1988 Photon emission with the scanning tunneling microscope *Z. Phys.* B **72** 497–501
[18] Coombs J, Gimzewski J, Reihl B and Sass J 1988 Photon emission experiments with the scanning tunnelling microscope *J. Microsc.* **152** 325–36
[19] Johansson P, Monreal R and Apell P 1990 Theory for light emission from a scanning tunneling microscope *Phys. Rev.* B **42** 9210–3
[20] Berndt R, Gimzewski J K and Johansson P 1991 Inelastic tunneling excitation of tip-induced plasmon modes on noble-metal surfaces *Phys. Rev. Lett.* **67** 3796–9
[21] Bharadwaj P, Bouhelier A and Novotny L 2011 Electrical excitation of surface plasmons *Phys. Rev. Lett.* **106** 226802
[22] Grigorenko A N, Polini M and Novoselov K S 2012 Graphene plasmonics *Nature Photon.* **6** 749–58
[23] Chen J *et al* 2012 Optical nano-imaging of gate-tunable graphene plasmons *Nature* **487** 77–81
[24] Fei Z *et al* 2012 Gate-tuning of graphene plasmons revealed by infrared nano-imaging *Nature* **487** 82–5
[25] Koppens F H L, Chang D E and García de Abajo F J 2011 Graphene plasmonics: a platform for strong light-matter interactions *Nano Lett.* **11** 3370–7
[26] Chen C F *et al* 2011 Controlling inelastic light scattering quantum pathways in graphene *Nature* **471** 617–20

[27] Schlaf R, Murata H and Kafafi Z H 2001 Work function measurements on indium tin oxide films *J. Electron Spectrosc. Relat. Phenom.* **120** 149–54
[28] Giovannetti G, Khomyakov P A, Brocks G, Karpan V M, van den Brink J and Kelly P J 2008 Doping graphene with metal contacts *Phys. Rev. Lett.* **101** 026803
[29] Brar V W 2010 Scanning tunneling spectroscopy of graphene and magnetic nanostructures *PhD Thesis* University of California, Berkeley
[30] Ferrari A C *et al* 2006 Raman spectrum of graphene and graphene layers *Phys. Rev. Lett.* **97** 187401
[31] Malard L M, Pimenta M A, Dresselhaus G and Dresselhaus M S 2009 Raman spectroscopy in graphene *Phys. Rep.* **473** 51–87
[32] Zhang Y, Brar V W, Wang F, Girit C, Yayon Y, Panlasigui M, Zettl A and Crommie M F 2008 Giant phonon-induced conductance in scanning tunnelling spectroscopy of gate-tunable graphene *Nature Phys.* **4** 627–30
[33] Moos G, Gahl C, Fasel R, Wolf M and Hertel T 2001 Anisotropy of quasiparticle lifetimes and the role of disorder in graphite from ultrafast time-resolved photoemission spectroscopy *Phys. Rev. Lett.* **87** 267402
[34] Tielrooij K J, Song J C W, Jensen S A, Centeno A, Pesquera A, Zurutuza Elorza A, Bonn M, Levitov L S and Koppens F H L 2013 Photoexcitation cascade and multiple carrier generation in graphene *Nature Phys.* **9** 248–52
[35] Brida D *et al* 2013 Ultrafast collinear scattering and carrier multiplication in graphene *Nature Commun.* **4** 1987
[36] Yu Y-J, Zhao Y, Ryu S, Brus L E, Kim K S and Kim P 2009 Tuning the graphene work function by electric field effect *Nano Lett.* **9** 3430–4